Constrained deformation of an Al based amorphous alloy by cold rolling

P. Rizzi[*], A. Habib, A. Castellero, L. Battezzati

Dipartimento di Chimica IFM and NIS, Università di Torino, V. Giuria 7, 10125 Torino, Italy

ARTICLE INFO

ABSTRACT

In this work, we report on the mechanisms of deformation and fracture of an $Al_{87}Ni_7La_6$ amorphous alloys by cold rolling. Ribbons were cold rolled at room temperature embedded in pure Al-foils (volume fraction 20%). Scanning Electron Microscopy observations of the cross section of the deformed samples revealed that, after a few rolling passes, ribbons broke into fragments and formed shear bands because of the load exerted by the ductile Al matrix starting from the roughness on the surfaces. The shear band offset was higher near the fracture surface, suggesting that a stress concentration occurs when the slip of shear band is hindered by the presence of constraint. In ribbons rolled alone elongation above 3% was achieved as well as flattening of the surface roughness.

Fracture surfaces of ribbon fragments presented mainly features due to brittle shear and a limited number of veins and filaments suggesting mixed mode of fracture.

No formation of crystals in the shear bands was evidenced by Transmission Electron Microscopy and Differential Scanning Calorimetry.

© 2011 Elsevier B.V. All rights reserved.

1. Introduction

With the advent of bulk metallic glasses, the mechanical properties of amorphous alloys could be studied with conventional techniques being the subject of intensive research [1]. A clear outcome of works in this field is that ductilisation of otherwise brittle metallic glasses can be achieved when the glass is deformed while constrained inside a suitable cage or container. The deformation takes place via the activity of numerous shear bands within the glass which find an obstacle to their propagation in the constraining medium. An example of this being the formation of shear bands underneath an indenter tip. A similar effect was found also in multilayers made by alternating a soft La-based glass with a hard Zr-based glass which showed extensive shear banding within the soft layers [2]. Also, studies on the deformation of nanocrystalline-amorphous nanolaminates obtained by sputtering [3–5] showed suppression of shear bands formation in the amorphous layer, large tensile ductility and nearly ideal plastic flow behaviour when the crystalline layers were thick enough to block the shear band.

The high strength of metallic glasses suggests that they could be considered as reinforcement in metal matrix composites. In early examples, ribbons were employed as aligned fibres in various matrixes: $Fe_{42}Ni_{42}B_{16}$ in Ni [6], $Ni_{78}Si_{10}B_{12}$ in Cu [7], and $Ni_{91}Si_7B_2$ in Cu–30Zn brass [8,9]. In tensile testing all these, it was recognized that the glassy reinforcement could be deformed to a substantial extent while constrained inside the matrix made of a ductile element or alloy. The strength of the composites followed the rule of mixtures. An Al-based composites made by warm pressing powders of Al and a powdered $Al_{85}Y_8Ni_5Co_2$ ribbon improved the plastic properties of the matrix according to the iso-stress model, instead [10]. In all cases an effect of reinforcement deformation was apparent.

In this work the repeated co-rolling of stacked layers of an Al-based glass embedded in a pure Al matrix, i.e. a simulated composite, is reconsidered in more depth with emphasis on the constrained deformation of the amorphous component at room temperature. The shear banding and fracture are studied statistically. A comparison is made with the same material rolled in the absence of the Al-matrix.

2. Experimental

Ribbons of $Al_{87}Ni_7La_6$ were produced by melt spinning under argon atmosphere resulting amorphous to X-ray diffraction. Cold rolling was performed with a twin roller apparatus (rollers of 75 mm in diameter) employing a constant linear speed of 0.012 m/s at room temperature ($T/T_g = 0.6$, with T_g = glass transition temperature) in two modes: (i) ribbon pieces about 2 cm long and about 40 μm thick were inserted between two pure Al foils 100 μm thick and 2 cm long. The volume fraction of glassy alloy with respect to Al was 20%. The whole stack was contained in a stainless steel envelope which was then rolled. The composites were extracted from the envelope and folded several times. (ii) Ribbons were inserted in the same envelope and cold rolled alone, without folding. The stainless steel foils were hardened beforehand by rolling. The opening of the roll gap was controlled to limit the deformation of the steel foils which are intended to transmit the load to the samples.

Five $Al_{87}Ni_7La_6$ samples were cold-rolled with Al foils (19 rolling passes and 3 foldings; 40 rolling passes and 3 foldings; 21 rolling passes and 6 foldings; 15 rolling passes and 7 foldings) and four were cold rolled alone (6 rolling passes; 12 rolling

* Corresponding author. Tel.: +39 0116707565; fax: +39 0116707855.
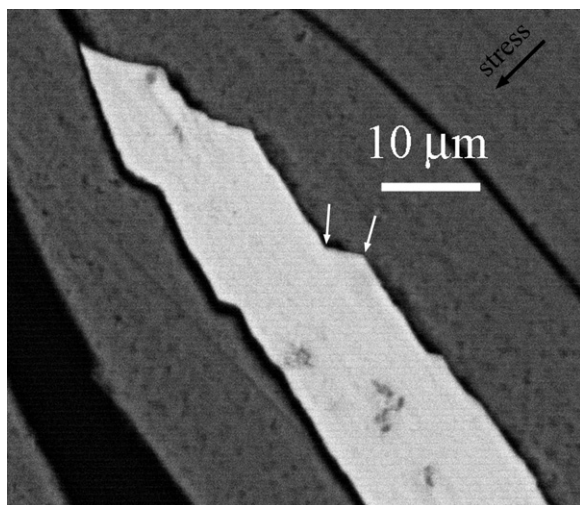*E-mail address:* paola.rizzi@unito.it (P. Rizzi).

Fig. 1. SEM backscattering electron image of the cross section of a sample after 40 rolling passes and 3 foldings: $Al_{87}Ni_7La_6$ appears light gray and the Al pure foils dark. White arrows point to shear offsets caused by the stress component along the direction marked with a black arrow. Rolling direction is perpendicular to the image plane.

Fig. 2. The shear bands offset versus $d/d_{1/2}$ (distance from the fracture surface divided by half of the total ribbon width) for all composite samples.

passes; 30 rolling passes; 41 rolling passes). In the latter case, the elongation was determined by measuring the sample length before (l_0) and after (l) deformation and assuming plane strain conditions during rolling so that the strain (ε) is $\varepsilon = \ln(l/l_0)$. Considering the sample length, an upper limit for the strain rate was estimated to $0.4\,s^{-1}$. From a shear rate versus T/T_g map [1], it is expected that inhomogeneous deformation occurs in these experimental conditions.

The surface and cross section of samples as well as ribbon fragments extracted from the Al foils were examined by Scanning Electron Microscopy (SEM). Differential Scanning Calorimetry (DSC) was used with samples before and after cold rolling to check for any change in the thermal stability due to the mechanical deformation. Transmission Electron Microscopy (TEM) studies were performed on fragments to check for the presence of crystals formed during deformation. They did not need thinning because their edges were thin enough to be transparent to the electron beam.

3. Results and discussion

The samples examined in this work display distinct behaviour according to whether Al crystalline foils were employed or not. Co-rolling of pure Al foils and amorphous $Al_{87}Ni_7La_6$ ribbons causes the fracture of ribbons into small fragments, independent from the number of passes and foldings so that all samples had similar appearance. The Al foils were reduced in thickness as seen in cross sections, with strain in excess of at least 40% embedding the fragments. Therefore, the strain of the entire sample cannot be defined and, in the following, general results will be presented referring to all of them.

Melt quenched ribbons do not have uniform section because of surface imperfections caused by wheel roughness and entrapped gas bubbles on the wheel side and liquid waves on the opposite side. When rolled alone, they elongate to some extent and show a decrease in surface roughness on increasing deformations (i.e. rolling passes). The strain of these ribbons can then be expressed in terms of elongation and also by means of the modification of the surface roughness as detailed in Section 3.2.

3.1. Ribbons rolled between Al foils

SEM analyses made on cross sections of $Al_{87}Ni_7La_6$ amorphous alloy/Al stacks show that the Al foils stick to each other but ribbons hardly adhere to them (Fig. 1). In the few examples reported in the literature on composites containing metallic glasses, the adhesion of the ribbon to the matrix was enabled by deposition on its surface of a crystalline metal (electroplating of Ni [6] or Cu [7] or
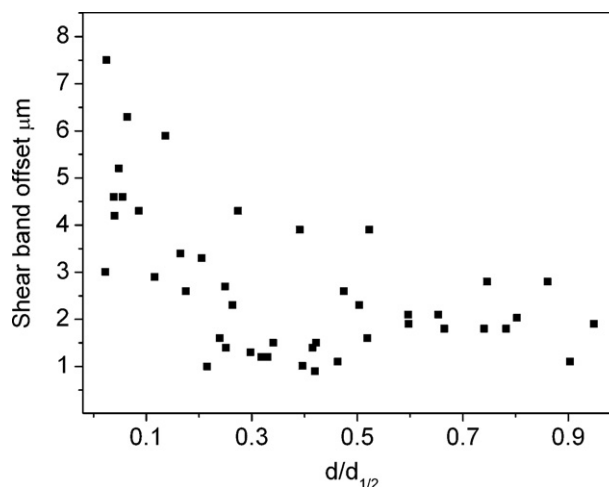
soldering with $Sn_{60}Pb_{40}$ [8,9]) followed by annealing to promote diffusional bonding between the matrix and the deposited layer. When amorphous ribbons of different compositions were rolled together ($Mg_{55}Cu_5Gd_{10}/Al_{87}Ni_7Gd_6$ and $Mg_{55}Cu_5Gd_{10}/Al_{87}Ni_7Y_6$) [11] welding was achieved in limited areas of the samples. On the other hand, in previous works [12,13] it was observed that during the rolling of alternated layers of Al and Ni, interdiffusion took place and the two metals stack together allowing the formation of intermetallic phases at the interfaces between the layers on low temperature annealing. This lack of adhesion seems to be due to the difference in ductility between the two components. It ensures, however, that the composition of the amorphous alloy did not change after processing.

In the SEM image of Fig. 1 (40 rolling passes and 3 foldings) the ribbon appears fractured in various points and severely deformed as a consequence of the formation of multiple shear bands. A large reduction in thickness is observed (from the $40\,\mu m$ of the undeformed ribbons to about $10\,\mu m$). Reduction in width is also found due to fracture and production of small fragments. Shear bands responsible for deformation and fracture are parallel to the deformation direction. Their shear offsets were measured for all samples and reported versus $d/d_{1/2}$ (distance from the fracture surface divided by half of the total ribbon length) (Fig. 2) finding that larger shear offsets occurred near the side where a critical shear band fractured the ribbon. Moving away from the fracture surface, the extent of the offset is reduced and remains almost constant with values ranging from 0.5 to $3\,\mu m$. When the deformation is applied under constraint, as in the present case of cold rolling, the slip of a shear band is hindered by the constraints and a stress concentration in weak regions occurs. This can induce larger offsets for the subsequent shear bands, finally causing fracture (i.e. the formation of a critical shear band). In fact, the pure Al, having much lower yield strength than the amorphous $Al_{87}Ni_7La_6$ alloy, deforms plastically on rolling and adapts to the roughness of the surface (i.e. mostly the cavities due to entrapped gas bubbles). Therefore, a stress concentration builds up in these thinner parts of the ribbon causing the high number of fracture events observed after a few rolling passes.

If stress concentration facilitates the formation of subsequent shear bands, it could be expected that the shear offset be proportional to the number density of the shear bands formed. Therefore, the interband spacing (λ) was measured versus $d/d_{1/2}$ (Fig. 3), and, contrary to expectations, a clear dependence was not detected. Since indentation can be considered as a deformation under constraint, in order to interpret these data the literature concerning the formation of shear bands underneath the indenter was examined.
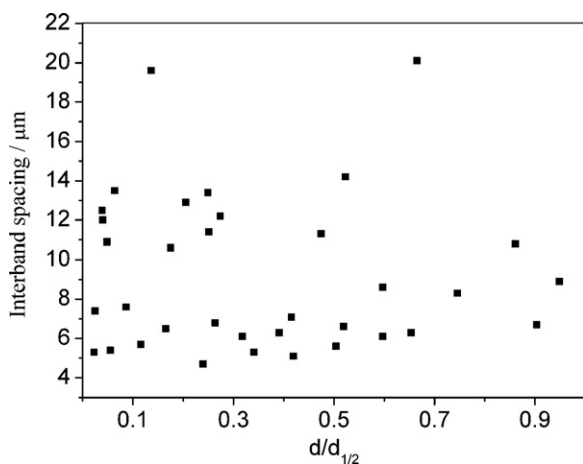
Fig. 3. The interband spacing versus $d/d_{1/2}$ (distance from the fracture surface divided by half of the total ribbon width) for all composite samples.

In [14] the interband spacing versus distance from the indenter tip was reported showing a decrease of λ in two regions where an extensive plastic deformation acted. At variance, Xie et al. reported that λ increases linearly with increasing distance from the indenter tip and the shear offset follows the same behaviour, being larger near the indenter tip [15]. When indentation was performed on samples previously plastically deformed, only scattered values were obtained. In our work, each successive rolling pass causes deformation, so that the spacings of Fig. 3 derive from shear bands formed in different stages of rolling, therefore, the scattered points in the λ versus distance plot appear to reproduce the findings in [15].

To have a further insight into the deformation of the ribbons, fragments extracted from the Al foils were examined by SEM (Fig. 4a and b). Shear bands were found in different directions showing that the ribbons underwent a large amount of deformation and fractured several times. In a previous work [16], a tensile test
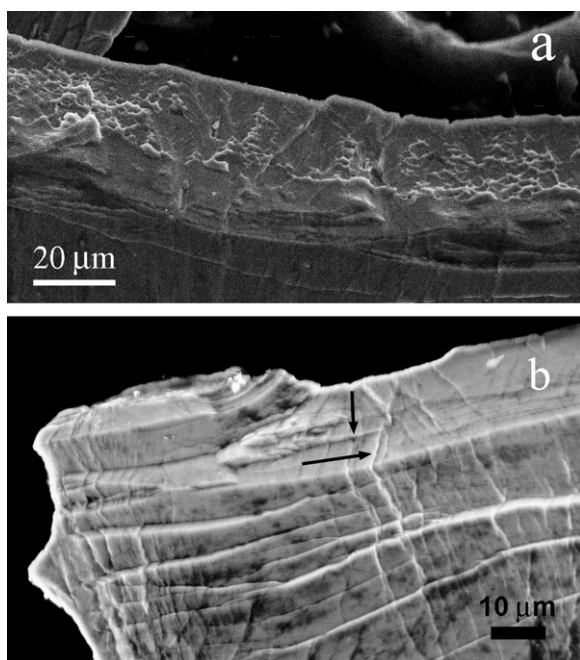

Fig. 4. SEM secondary electron images of fragments of a sample after 40 rolling passes and 3 foldings: (a) fracture surface with veins; (b) flat fracture surface. Arrows indicate an example of perpendicular shear offsets.
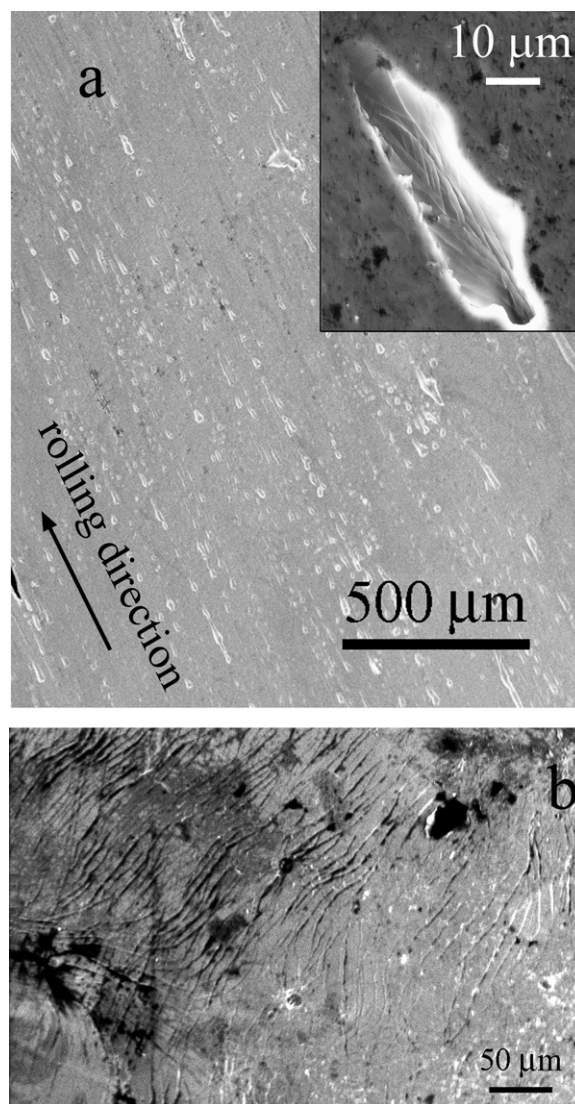

Fig. 5. SEM secondary electron images of surfaces of ribbons in: (a) sample after 6 rolling passes; (b) a sample after 41 rolling passes.

of $Al_{87}Ni_7La_6$ amorphous ribbons was performed in which catastrophic failure of the sample occurred immediately after the elastic regime with formation of a low number of shear bands. A typical vein pattern was observed on fracture surfaces in that case, with protuberances or filaments emerging from the veins. This microstructure can be associated to an increase in temperature above the glass transition during the shear band slip. In the cold rolled samples studied here, some fracture surfaces displayed veins but more often they contained series of shear offsets of various length to which such a rise in temperature cannot be associated. In the fracture surface shown in Fig. 4a, a smooth shear offset is seen indicating where failure started as suggested in [17–19], followed by a vein patterned area covering the majority of the surface. In Fig. 4b a further fracture surface is shown in which two sets of shear offsets, perpendicular to each other, very likely formed in subsequent rolling passes. At first, the smooth area was formed due to cleavage and then the perpendicular offset occurred (see arrows) during further deformations. Overall, a mixed mode of fracture is observed in rolled fragments: predominant brittle shear and some vein tearing.

TEM images of fracture surfaces in a sample submitted to tensile testing did not display any evidence of crystallisation [16]. In

this work, the edge of ribbon fragments extracted from Al foils was examined by TEM and no crystals were detected as well. Moreover, no change in the crystallisation behaviour was found in DSC analyses made with un-rolled and rolled samples, being DSC peaks completely overlapped. There is still debate in the literature on the cause of crystallisation in shear bands during deformation. In Al-Ni-Y and Al-Fe-Gd alloys Jiang and co-workers [20,21] show that nanocrystals are formed within shear bands during bending in the part of the specimen undergoing compression, but no crystallisation is detected in the part in tension. We find for amorphous $Al_{87}Ni_7La_6$, that neither compression nor tension [16] leads to crystallisation.

3.2. Ribbons rolled alone

For comparison with the above findings, $Al_{87}Ni_7La_6$ amorphous ribbons were cold rolled alone increasing progressively the number of rolling passes and, therefore, increasing the elongation (6 rolling passes, $\varepsilon = 0.011$; 12 rolling passes, $\varepsilon = 0.013$; 30 rolling passes $\varepsilon = 0.029$; 41 rolling passes 0.033). After 6 rolling passes the ribbon wheel side still showed the presence of cavities (Fig. 5a) in which shear offsets are evident, as shown in the insert of Fig. 5a. Although the overall elongation of this sample was small, deformation must have concentrated locally with higher strain. At this stage no evidence of cracks was found. After 41 rolling passes (Fig. 5b) cavities almost disappeared and shear bands were evident on both ribbon surfaces, that could not be distinguished anymore, and cracks appeared where surface imperfections were present in the as quenched sample although it did not fracture yet. Shear bands are both perpendicular and parallel to the rolling direction.

In order to follow the increase in deformation, the longitudinal and lateral size of cavities were measured for all samples finding an apparent decrease of both as a function of the number of rolling passes together with a decrease in their total number. When rolling ribbons alone, the stress distribution differs from the composite case. In fact, the maximum stress is imposed by the constraint of steel foils to the thicker part of the ribbon, that plastically deforms via shear bands, filling the cavities that are progressively reduced in size and consequently in depth.

4. Conclusions

This paper presents results on the constrained deformation of $Al_{87}Ni_7La_6$ amorphous ribbons at room temperature by rolling either composite samples made of amorphous $Al_{87}Ni_7La_6$/Al foils and ribbons alone. No evidence of crystallisation was found in either case. Ribbons rolled alone plastically deformed, via shear bands, showing some elongation in the rolling direction and reduction in surface roughness that was almost cancelled at 0.033 strain.

When composites were cold rolled, the ductile Al adapted to the surface roughness so that a stress concentration set up in the cavities, i.e. the weaker parts of the ribbon, that were fractured in small fragments. A large amount of shear bands was found both parallel and perpendicular to the deformation direction. Larger shear offsets were found near the fracture surface and were attributed to the effect of the stress concentration at weak points after the constraints hindered the slip of previously formed shear bands. The interband spacing did not show a clear dependence on position, probably due to the successive deformation undergone in each rolling pass that enable the formation of secondary shear bands in samples already deformed.

SEM studies of ribbon fragments evidenced mostly the occurrence of brittle fracture surfaces and to a limited extent of vein patterns indicating that mostly cold shear bands were operative.

DSC measurements on both samples rolled alone and composites revealed that no significant changes in the thermal stability appear after deformation, suggesting that during deformation there was no detectable formation of nanocrystals in the shear bands as confirmed by TEM.

References

[1] C.A. Schuh, T.C. Hufnagel, U. Ramamurty, Acta Mater. 55 (2007) 4067.
[2] P. Sharma, K. Yubuta, H. Kimura, A. Inoue, Phys. Rev. B 80 (2009) 024106.
[3] A. Donohue, F. Spaepen, R.G. Hoagland, A. Misra, Appl. Phys. Lett. 91 (2007) 241905.
[4] Y. Wang, J. Li, A.V. Hamza, T.W. Barbee, Proc. Natl. Acad. Sci. USA 104 (27) (2007) 1115.
[5] M.C. Liu, J.C. Huang, H.S. Chou, Y.H. Lai, C.J. Lee, T.G. Nieh, Scr. Mater. 61 (2009) 840.
[6] M. Blank-Bewersdorff, U. Köster, G. Steinbrink, J. Mater. Sci. Lett. 8 (1989) 796.
[7] A.T. Alpas, J.D. Embury, Scr. Met. 22 (1988) 265.
[8] Y. Leng, T.H. Courtney, J. Mater. Sci. 24 (1989) 2006.
[9] Y. Leng, T.H. Courtney, J. Mater. Sci. 26 (1991) 588.
[10] S. Scudino, K.B. Surreddi, S. Sager, M. Sakaliyska, J.S. Kim, W. Löser, J. Eckert, J. Mater. Sci. 43 (2008) 4518.
[11] J.S. Park, J.M. Kim, E.S. Park, Intermetallics 18 (2010) 1920.
[12] L. Battezzati, P. Pappalepore, F. Durbiano, I. Gallino, Acta Mater. 47 (1999) 1901.
[13] L. Battezzati, C. Antonione, F. Fracchia, Intermetallics 3 (1995) 67.
[14] R. Bhowmick, R. Raghavan, K. Chattopadhyay, U. Ramamurty, Acta Mater. 54 (2006) 4221.
[15] S. Xie, E.P. George, Acta Mater. 56 (2008) 5202.
[16] P. Rizzi, L. Battezzati, J. Non-Cryst. Solids 344 (2004) 94.
[17] C. Ma, A. Inoue, Mater. Trans. JIM 43 (2002) 3266.
[18] Z.F. Zhang, J. Eckert, L. Schultz, Acta Mater. 51 (2003) 1167.
[19] V.Z. Bengus, E.D. Tabachnikova, J. Miskuf, K. Csach, V. Ocelik, W.L. Johnson, V.V. Molokanov, J. Mater. Sci. 35 (2000) 4449.
[20] W.H. Jiang, M. Atzmon, Acta Mater. 51 (2003) 4095.
[21] W.H. Jiang, F.E. Pinkerton, M. Atzmon, Acta Mater. 53 (2005) 3469.